Wetting Transitions in a Cylindrical Pore

Andrea J. Liu, D. J. Durian, Eric Herbolzheimer, and S. A. Safran

Exxon Research and Engineering Company, Route 22 East, Annandale, New Jersey 08801

(Received 26 March 1990)

The wetting behavior of two-phase systems confined inside cylindrical pores is studied theoretically. The confined geometry gives rise to wetting configurations, or microstructures, which have no analog in the well-studied planar case. Many features observed in experiments on binary liquid mixtures in porous media, previously interpreted in terms of random fields, are shown to be consistent with wetting in a confined geometry with no randomness.

Binary liquid mixtures inside porous media have attracted considerable attention because of their rich behavior, potential applications, and proposed connection[1] to the random-field Ising model. Experiments on such systems[2-5] display a variety of results, but two general features consistently emerge: (i) There is metastability and, correspondingly, strong history dependence, deep within the two-phase region; and (ii) macroscopic phase separation does not occur, even far inside the coexistence region of the bulk mixture. Although these features are qualitatively consistent with the random-field model, they are typically observed far from the bulk critical point, where the model is not expected to apply.[1] Here, we directly consider the phenomenon of wetting, which plays an important role in porous media. It is notoriously difficult, however, to characterize the contorted geometries of porous media, which, in turn, must influence the wetting behavior.[6] We have ventured away from the well-studied planar case[7] by examining wetting in an idealized geometry, namely, a single cylindrical pore. We have derived a wetting phase diagram and have found that the experimentally observed features, (i) and (ii) above, are qualitatively consistent with our model, which contains *no randomness*.

Previous theoretical work on two-phase systems in cylindrical pores has focused on the phenomenon of capillary condensation,[8] where the pore fills up with a single phase rich in the wetting component. A confined geometry in contact with a bulk reservoir at two-phase coexistence will contain only this single, wetting phase. To achieve two-phase coexistence *inside* a confined geometry, we impose the constraint of constant overall composition (as in experiments on binary liquid mixtures confined in sealed Vycor samples[5]), and obtain an analog of the wetting transition. Since the constraint requires the system to be finite, the phase transitions we encounter are rounded.

A summary of our results for a cylindrical pore of radius r_0 and length $L \gg r_0$ filled with a binary liquid mixture is given by the wetting phase diagram of Fig. 1. We assume throughout the case of fixed critical composition and symmetric coexistence curve, so that the volume fraction occupied by each phase is $\frac{1}{2}$. In equilibrium,

there are two possible configurations, corresponding to complete and partial wetting. The complete-wetting configuration consists of a single bubble of length l and radius r_c of the nonwetting phase β suspended in the center of the pore. The bubble is surrounded by the wetting phase α which coats the inside surface of the pore. The partial-wetting configuration consists of regions of α and β, each of length $L/2$, separated by an α-β interface stretching across the pore. The *short* capsules and plugs depicted in Fig. 1 are long lived in that they coarsen slowly with time. The possible connection of these configurations to experimental observations will be discussed later.

A phenomenological calculation for the case of contact forces, along the lines of Cahn's argument,[9] showed that the wetting transition temperature moves closer to criticality in the cylindrical geometry.[10] A more realistic ap-
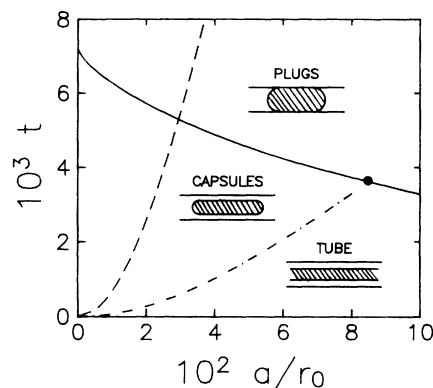

FIG. 1. Wetting phase diagram for a binary liquid mixture confined in a cylindrical pore of radius r_0, as a function of reduced temperature [$t = (T_c - T)/T_c$ is positive in the two-phase region] and inverse pore radius, a/r_0, where a is a molecular length. The three configurations of tubes, capsules, and plugs are sketched (with the nonwetting phase hatched in), along with the wetting transition (solid curve). Also shown are the boundary between capsules and the tube (dot-dashed curve) and the $\Delta = 0$ hydrodynamic stability boundary of the tube (dashed curve). For small pores there is a direct transition between plugs and the tube, while for larger pores there is an intermediate capsule regime.

proach, adopted here, is to include an effective interface potential which decays away from the pore wall and to calculate the corresponding wetting phase diagram. We begin by constructing the free energies per unit length along the pore (F_{cw} and F_{pw}) for the two configurations (complete and partial wetting). We assume that the correlation length of the liquid mixture is not large compared to the pore radius, so that a well-defined α-β interface exists.[11] Thus, we find that the free energies per length of the configurations are given by

$$F_{cw}/2\pi = \varphi_\beta r_0^2 [\sigma + \overline{A}V(r_c)]/r_c , \tag{1}$$

$$F_{pw}/2\pi = \tfrac{1}{2}\varphi_\beta \overline{A}_2 r_0 . \tag{2}$$

Here, $\varphi_\beta = \tfrac{1}{2}$ is the volume fraction occupied by the β phase, σ is the α-β interfacial tension, $\overline{A}V(r)$ is the effective interface potential, or free energy per unit area, as a function of the inner radius r, and $\overline{A}$ and $\overline{A}_2$ are temperature-dependent Hamaker constants corresponding, respectively, to the interface potential and the free-energy difference of filling the pore with β instead of α. The bubble radius r_c is determined by the competition between wetting forces, which favor a small radius, and surface tension, which favors a large radius. We obtain r_c by minimizing (1) and solving

$$\sigma + \overline{A}\left[V(r_c) - r_c\frac{dV}{dr}\bigg|_{r_c}\right] = 0 . \tag{3}$$

The bubble length l is then fixed by the volume constraint $r_c^2 l = \varphi_\beta r_0^2 L$. There is an upper bound on the length, $l \le L$, or equivalently, a lower bound on the radius, $r_c \ge r_t$, where

$$r_t = \sqrt{\varphi_\beta} r_0 . \tag{4}$$

We assume throughout that the wetting forces are van der Waals in character and use $V(r)$ and F_{pw} calculated within a pair-potential approximation.[12] (Nevertheless, we expect the phase diagram to be qualitatively the same for forces which decay more rapidly than van der Waals forces.) We have introduced a molecular cutoff a to prevent an unphysical divergence at $r = r_0$; in that limit $V(r)$ then approaches $1/(r - r_0 + a)^2$, the planar result.

The Hamaker constants and interfacial tension all vanish at the critical point. The former vary with temperature as $\overline{A} \approx At^\beta$ and $\overline{A}_2 \approx A_2 t^\beta$, and the interfacial tension varies as $\sigma \approx \sigma_0 t^\mu$, where $t = (T_c - T)/T_c$. Note that t is positive in the two-phase region considered here. The parameters A, A_2, and σ_0 are material dependent; in Fig. 1, we adopt $A/\sigma_0 a^2 = 0.05$ and $A_2/A = 0.4$.[13] We also use the exponent estimates $\mu = 1.264 \pm 0.002$ and $\beta = 0.328 \pm 0.004$.[14]

With these ingredients, we obtain the wetting transition drawn as a solid line in Fig. 1 by equating numerically the free energies per length of the complete- and partial-wetting configurations as a function of temperature and pore radius. Physically, the transition arises

from the competition between surface tension and wetting forces. Near the critical point, surface tension is the weaker of the two because the exponent μ is larger than β; but the balance shifts as the temperature moves away from criticality. We find that the wetting transition is first order for realistic values of the parameter A_2/A and moves closer to the bulk critical point as the pore size decreases.

With the equilibrium wetting transition now in hand, we turn to new configurations characteristic of the nonequilibrium behavior. In the partial-wetting case, we consider long-lived "plug" configurations as shown in Fig. 1, where a series of α-β interfaces stretch across the pore to form short alternating plugs of the two phases. In the complete-wetting case, we find a distinction between two configurations: the long-lived "capsule" configuration, consisting of a series of bubbles of the β phase along the length of the pore, and the equilibrium "tube" configuration. In the latter, the wetting force is so strong that the β phase forms one long cylindrical bubble in the center of the pore, with a radius given by the lower bound r_t in Eq. (4) above.

The boundary between the capsule and tube configurations is given by the dot-dashed line in Fig. 1. We find the tube configuration when the wetting force is strongest relative to surface tension, i.e., near the critical point. As the boundary is approached from the capsule side, the wetting force squeezes the capsule radius until the capsules are forced to coalesce into the tube, which cannot be squeezed further. Thus, the capsule-tube boundary is reached when r_c approaches its lower bound: $r_c = r_t$, where r_c satisfies (3) and r_t satisfies (4).[15] Evidently, the boundary is a direct consequence of the constraint of constant composition, and is not a true phase transition. Note that for sufficiently small pores, the wetting force is so strong that there is a direct transition between plugs and the tube. For larger pores, however, the intermediate capsule configuration appears.

We now consider how the long-lived capsule and plug configurations can arise. One possibility is that they might be formed by nucleating droplets after a quench from the single-phase region into the capsule or plug regimes. In this case, we would expect the length of the resulting capsules and plugs to be on the order of the pore radius. A second possibility is that capsules or plugs could form from a Rayleigh-like instability of the tube configuration, in which the cylinder of the β phase breaks up into droplets to reduce its surface area. In contrast to the case of an isolated cylinder where there is always a Rayleigh instability, the new twist here is that wetting forces from the pore walls can counter the destabilizing effect of surface tension. From an energetic argument, we find that a cylinder of the β phase of radius r enclosed in the pore is stable against small sinusoidal perturbations of the radius if $\Delta(r) > 0$, where

$$\Delta(r) \equiv \overline{A}\frac{d^2V}{dr^2} - \frac{\sigma}{r^2} . \tag{5}$$

For a long bubble of equilibrium length and radius r_c given by (3), the condition $\Delta(r_c) > 0$ is always satisfied and, consequently, an equilibrium bubble is *always stable*. Now consider the stability of the tube configuration with radius r_t given by (4). The condition $\Delta(r_t) = 0$ is shown as a dashed line in Fig. 1; at reduced temperatures below the curve, the wetting forces are strong enough to prevent the Rayleigh instability. Thus, the tube configuration is always stable in the tube regime, below the dot-dashed line in Fig. 1. Experimentally, a metastable tube of radius r_t can be created by a fast temperature quench from the tube regime to the capsule regime. If the quench is slow then the radius can adjust smoothly to its new equilibrium value, $r_c > r_t$ given by (3), by draining the wetting layer of a. But if the quench is faster than the drainage time,[16] the tube can remain hydrodynamically stable up to the dashed line in Fig. 1, beyond which it will break up into shorter capsules or plugs.

In order to estimate the *size* of the capsules or plugs resulting from the breakup of the tube, we must go beyond energetics and study the dynamics by solving the linearized Navier-Stokes equation with moving boundary conditions. For a perturbation of the radius $e^{iqz+\omega t}$, where z measures distance along the pore, the resulting dispersion relation is

$$\omega \propto -q^2[\Delta(r_t) + \sigma q^2], \qquad (6)$$

where $\Delta(r)$ is again given by (5). When $\Delta < 0$ the tube is unstable, and the wavelength of the fastest growing mode is $\lambda_{max} = 2\pi r_0(2\sigma/\Delta r_0^2)^{1/2}$. This provides a rough estimate of the length of the capsules or plugs. The dependence of λ_{max} on Δ, or equivalently the quench depth, shows that our model predicts a history-dependent length distribution of capsules and plugs. This is consistent with the experimental observations of metastability deep in the two-phase region. For example, history-dependent structure factors have been seen in several scattering experiments.[3,17] Moreover, since the scale of λ_{max} is set by r_0, our model predicts that a fast quench yields phase-separated domains on a scale of the pore size, rather than on a macroscopic scale. Note that this differs from the random-field prediction that the domain size and the thickness of the α-β interface should be the same.

To see why complete phase separation is realistically *prohibited* in our model, we have estimated the time scale for the short domains to coarsen after being created by a fast quench. For plugs and capsules, the usual mechanism of Ostwald ripening is inhibited because their curvatures, and hence Laplace pressures, are nearly independent of their length; we therefore expect plugs to coarsen extremely slowly. The capsule phase, on the other hand, is able to coarsen by the coalescence of individually diffusing capsules. By estimating the drag on a capsule in a pore of radius r_0, we find the coalescence time for capsules of radius r and length l to diffuse by

the distance of their spacing to be given by $\tau_c \propto l^3/(r_0 - r)^2$. For capsules with $r/r_0 = 0.9$ and l comparable to the wavelength of light (say, 5000 Å) in a 30-Å-radius pore, the coalescence time is on the order of an hour. (The resulting 1-μm-long capsules will take 8 h to coalesce into 2-μm capsules, and so on.) Thus, macroscopic phase separation is inhibited by kinetics. In addition, the capsule diffusion constant vanishes as r approaches r_0, or equivalently, as the reduced temperature t increases. Similar behavior was observed in dynamic light-scattering experiments on a binary liquid in Vycor,[5] where the internal dynamics slowed down as the temperature moved further into the two-phase region.

Many of these features may persist in Vycor, which consists of interconnected pores of average radius roughly 30 Å and length roughly 180 Å.[5] In order to make quantitative predictions, the presence of necks, connectivity of the pore space, and variation of pore radius must be considered. We expect, however, that configurations analogous to our tube, capsule, and plug microstructures will still arise,[18] and that transitions will still be governed by the competition between surface tension and wetting forces. Geometrical irregularities may help destabilize the tube configuration, depressing the tube-capsule transition to smaller reduced temperatures. The tortuous geometry should have a more dramatic effect on the kinetics; for example, it may alter the initial size of the capsules following a quench and add a further steric barrier to capsule coalescence.

We now discuss the extension of these ideas to related phenomena. Our approach to wetting in a pore can be applied to the outside of a cylindrical fiber. We find that the *equilibrium* wetting layer on a fiber is always hydrodynamically stable (as shown above, the same is true for a bubble of equilibrium radius). This result also holds for wetting forces which decrease more quickly with distance than the van der Waals force assumed here. Landau-Ginzburg calculations of wetting phase diagrams on the outside of a cylinder[19,20] were therefore justified in neglecting the Rayleigh instability. In the case of a wetting layer thicker than its equilibrium value, however, it has been shown[21,22] that a Rayleigh instability can occur.

Our approach also predicts new behavior in capillary condensation.[8] One typically studies a liquid-vapor system in a porous material in contact with a reservoir of fluid, as coexistence is approached from the single-phase region on the vapor side. At sufficiently small vapor pressures, the equilibrium configuration is a tube of vapor of radius r surrounded by a liquid layer which coats the pore wall. As the vapor pressure increases toward coexistence, this liquid layer thickens, and the hydrodynamic stability parameter $\Delta(r)$ [see (5)] decreases from its initial positive value until it reaches zero at a vapor pressure $p = p_a$, where the Rayleigh instability develops. At the same pressure $p = p_a$, a thermodynamic instability develops and molecules rush in from the vapor

reservoir to fill the pore with liquid.[12] If the Rayleigh instability develops faster than the thermodynamic instability, one might expect to see bubbles of vapor (similar to capsules) trapped in the liquid.

In conclusion, this work extends the theory of wetting on planar substrates to a confined geometry. In addition to the rich behavior characteristic of planar wetting transitions, several new features emerge as a generic consequence of confinement. Thus, our picture captures salient aspects of wetting in true porous media, and should provide a useful framework and stimulus for future theoretical and experimental studies of wetting in porous media.

[1]F. Brochard and P. G. de Gennes, J. Phys. (Paris), Lett. 44, 785 (1983); P. G. de Gennes, J. Phys. Chem. 88, 6469 (1984).

[2]J. V. Maher, W. I. Goldburg, D. W. Pohl, and M. Lanz, Phys. Rev. Lett. 53, 60 (1984).

[3]S. K. Sinha, J. S. Huang, and S. K. Satija, in Scaling Phenomena in Disordered Systems, edited by R. Pynn and A. Skjeltorp (Plenum, New York, 1985), p. 157; J. S. Huang, S. K. Sinha, W. I. Goldburg, J. V. Maher, and S. K. Satija, Physica (Amsterdam) 136B, 291 (1986).

[4]M. C. Goh, W. I. Goldburg, and C. M. Knobler, Phys. Rev. Lett. 58, 1008 (1987); W. I. Goldburg, in Physics of Complex and Supermolecular Fluids, edited by S. A. Safran and N. A. Clark (Wiley, New York, 1987), p. 475.

[5]S. B. Dierker and P. Wiltzius, Phys. Rev. Lett. 58, 1865 (1987); P. Wiltzius, S. B. Dierker, and B. S. Dennis, Phys. Rev. Lett. 62, 804 (1989).

[6]D. Ronis, Phys. Rev. A 33, 4319 (1986).

[7]See, e.g., P. G. de Gennes, Rev. Mod. Phys. 57, 827 (1985); D. E. Sullivan and M. M. Telo da Gama, in Fluid Interfacial Phenomena, edited by C. A. Croxton (Wiley, London, 1986), p. 72; S. Dietrich, in Phase Transitions and Critical Phenomena, edited by C. Domb and J. L. Lebowitz (Academic, London, 1988), Vol. 12, p. 1.

[8]See, e.g., R. Evans, U. Marini Bettolo Marconi, and P. Tarazona, J. Chem. Phys. 84, 2376 (1986); B. K. Peterson, K. E. Gubbins, G. S. Heffelfinger, U. Marini Bettolo Marconi, and F. van Swol, J. Chem. Phys. 88, 6487 (1988).

[9]J. W. Cahn, J. Chem. Phys. 66, 3667 (1977).

[10]D. J. Durian, Ph.D. thesis, Cornell University, 1989 (unpublished).

[11]We have neglected end-cap contributions, which vanish as r_0/L as the pore length L increases. This is justified because r_0/L can be made arbitrarily small.

[12]M. W. Cole and W. F. Saam, Phys. Rev. Lett. 32, 985 (1974); Phys. Rev. B 11, 1086 (1975).

[13]The value $A/\sigma_0 a^2 = 0.05$ was calculated for the specific case of nitromethane and carbon disulfide against glass. We used the Hamaker constant A estimated by R. F. Kayser [Phys. Rev. B 34, 3254 (1986)], and the surface-tension amplitude σ_0 derived from the correlation-length amplitude [X.-l. Wu, Ph.D. thesis, Cornell University, 1987 (unpublished)] via a universal amplitude ratio [see, e.g., M. R. Moldover, Phys. Rev. B 31, 1022 (1985)]. The ratio A_2/A should be of order unity and was arbitrarily chosen to be 0.4.

[14]M. E. Fisher and J.-H. Chen, J. Phys. (Paris) 46, 1645 (1985).

[15]The tube-capsule boundary is not well defined in that it depends (albeit weakly) on the length l of the metastable capsules, through the contribution of the end caps. Nevertheless, we have neglected such corrections, since we are not attempting to provide a precise quantitative description.

[16]For example, faster than a minute for a 100-Å-radius pore of aspect ratio 100. The drainage time varies with the pore radius r_0 and pore length l_0 as $\tau_d \propto l_0^2/r_0$.

[17]S. B. Dierker and P. Wiltzius (unpublished).

[18]J. K. Williams and R. A. Dawe, J. Colloid Interface Sci. 117, 81 (1987); 125, 347 (1988).

[19]M. P. Gelfand and R. Lipowsky, Phys. Rev. B 36, 8725 (1987).

[20]J. O. Indekeu, P. J. Upton, and J. M. Yeomans, Phys. Rev. Lett. 61, 2221 (1988); P. J. Upton, J. O. Indekeu, and J. M. Yeomans, Phys. Rev. B 40, 666 (1989).

[21]F. Brochard, J. Chem. Phys. 84, 4664 (1986).

[22]D. Quéré, J.-M. di Meglio, and F. Brochard-Wyart, Rev. Phys. Appl. 23, 975 (1988).